ANALYSIS OF THE UNSTEADY FLOW OF CENTRIFUGAL AGRICULTURAL AUTO WATER PUMPS WITH VARIABLE CURVATURES
/
变曲率离心式农用汽车水泵的非定常流动分析

Lect. Ph.D. Xue Dangqin [1], Lect. Ph.D. Ma Shibang [2*], Lect. Ph.D. Eng. Shi Huojie [3,4], Prof. Ph.D.Hou Shulin [4]
[1] School of Mechanical &Automotive Engineering, Nanyang Institute of Technology, Henan / China; [2] Nangyang Normal University, Henan / China; [3]Department of Biological Systems Engineering, Washington State University, Pullman/USA; [4] College of Engineering ,China Agricultural University, Beijing / China;
Tel: +8613782173858; Email: xqd5599@163.com

Abstract: *Existing research on agricultural auto water pumps mainly concentrate on structure optimization; nonetheless, a few works examine the characteristics of the inner flow field. The current study conducted an unsteady numerical simulation calculation of agricultural auto water pumps using an impeller model with a 0.5 mm blade tip clearance (σ) and ANSYS CFX software. The unsteady flow results were analyzed, and results indicated that the unsteady characteristics of the lift undergo significant periodic changes due to the dynamic and static interference of the cut water and the impeller. This change in frequency is in accordance with the passing frequency of the blade. The pressure fluctuation varies at different monitoring points on the same volute section. The pressure fluctuation decreases first and then increases from the bottom volute to the back volute. Additional dither components were also detected at the monitoring points on the bottom volute. The pressure fluctuation is maximized at the circumferential monitoring points proximal to the water cut. The distance between the circumferential monitoring points and the water cut increases with the circumference angle, whereas the fluctuation amplitude decreases. The results of fluid dynamics provide useful references to determine the reduction in the vibration and noise of agricultural auto water pumps.*

Keywords: *Agricultural auto water pumps; Pressure fluctuation; Unsteady flow; Variable-curvature*

INTRODUCTION

The market demand for agricultural automobiles has increased with social development. The agricultural auto water pump is a centrifugal pump that transmits medium energy based on a steady pressure difference generated under a certain flow rate. Nonetheless, unsteady flow occurs in different working conditions because of the high rotation speed of the water pump and the unsteady geometric boundaries of the rotating impeller. Furthermore, the inner fluid forms a boundary layer on the solid wall surface, which in turn causes interior backflow and interference from dynamic and static components, as well as leaking and wake flows at the blade tip. Moreover, the formation of the boundary layer results in the fluctuation of flow field pressure and the generation of an alternating acting force. In the process, resonance or fatigue damages are incurred [5,6]. For the effective operation of an agricultural auto water pump, strict requirements are proposed for its stability, although these requirements do not include the lift design requirements.

3-D unsteady numerical simulation technology is widely used because of the rapid development of computational fluid dynamics and computer technology. Both Chinese and foreign scholars conducted research on water pumps by combining test analysis and numerical simulation calculation [4,7,12]. For example, References

摘要: *目前对于农用汽车水泵的研究主要集中在结构优化上，而其内部流场特性研究较少。本文选择叶顶间隙 σ 为 0.5mm 的叶轮模型，采用 Ansys-CFX 软件对农用汽车水泵进行非定常数值模拟计算，分别研究在 Q/Qd=0.7、1 及 1.3 三种工况下的非定常压力脉动特性，并对非定常流动进行了结果分析。结果表明：由于隔舌与叶轮的动静干涉作用，扬程的非定常特性呈现明显的周期性变化，且频率和叶片通过频率一致。处于同一蜗壳断面不同位置的监测点的压力脉动幅度不同，从蜗壳底部向蜗壳背面先减小后增大，且位于蜗壳底部监测点的高频脉动成分较多。沿蜗壳周向，隔舌附近监测点压力脉动幅度最大，随着圆周角的增加，各监测点沿周向与隔舌距离变大，脉动幅值逐渐减小。从流体动力学方面对分析农用汽车水泵如何降低振动及噪声提供了有益的结果。*

关键词: *变曲率; 农用汽车水泵; 压力脉动; 非定常流动*

引言

随着社会的发展，农用汽车市场需求旺盛。农用汽车水泵作为一种离心泵通过某一流量下产生一个稳定的压力差达到输送介质能量的目的，但由于水泵转速高，旋转叶轮的几何边界是非定常的，在任何工况下运行都存在非定常流动，且内部流体在固体壁面上会形成边界层，会导致内部回流、动静部件干涉、叶尖泄漏流动、尾流，重要的是还会引起流场压力脉动并产生交变的作用力，导致产生共振或疲劳破坏[5,6]。因而为了保持农用汽车水泵的良好运行，除了满足扬程等设计要求外，对其稳定性的要求也越来越高。

随着计算流体力学 CFD(Computational Fluid Dynamics)和计算机技术的快速发展，三维非定常数值模拟技术已广泛应用，国内外学者已经对水泵进行了试验研究和数值模

[2, 10, 14] described the interaction between the impeller diffuser in a pump and pump performance; these works determined that the unsteady flow at the impeller exit is the main cause of pressure fluctuation. APRE et al. of Switzerland [3] studied inner flow in a draft tube of a mixed-flow water turbine model through a steady-state analysis of six different flow points under controlled working conditions. These researchers also analyzed fluctuation amplitude and frequency characteristics in a conical draft tube as well as vortex strip frequency and pressure fluctuation at small flow points under no-steam turbid. Reference [1] conducted high-frequency pressure sensor measurement proximal to the discharge flange of the centrifugal pump. The collected data were processed with fast Fourier transform, and the results indicate that the main signal frequency is the blade passing frequency of the centrifugal pump. This signal was used to measure the rotation speed of the pump. Reference [13] summarized the pressure fluctuation testing techniques used worldwide. The researcher tested the pressure fluctuation characteristics at the different impeller exit directions of the centrifugal pump and determined the relationship between unsteady fluid flow and pressure fluctuation at the impeller exit. The results indicated that the main causes of pressure fluctuation are the fluctuation in blade frequency induced at the efflux–wake and the shaft frequency fluctuation caused by asymmetric flow in the impeller passage. The pressure fluctuation caused by the structure declines with the widening of the distance between the impeller and the volute section. Moreover, a 100–145 Hz broadband frequency between four times the shaft and the blade frequencies was discovered in the spectrum of pressure fluctuation frequency at the blade exit. Charler [8] employed large-eddy simulation to calculate the pressure fluctuations in the volute, runner, and draft tube of a mixed-flow water turbine. By contrast, a few models employed a running simulation approach that cannot set real boundary conditions at the entrance of the draft tube. Although the average inflow conditions can be selected, the calculated flow state of the draft tube remains unsteady. The pressure fluctuation test in a draft tube mainly focuses on pressure fluctuation amplitude and frequency characteristics. Internal situations are impossible to observe; therefore, pressure fluctuation amplitude must be computed and the causes of pressure fluctuation analyzed.

The current study used the RNG k-*ε* turbulence model and conducted an unsteady numerical simulation of the full flow path for a quadratic, variable-curvature, half-open, and centrifugal agricultural auto water pump. The unsteady pressure fluctuation characteristics in such a path were analyzed when Q/Q_d = 0.7, 1.0, and 1.3. The results have strong practical significance for determining how pressure fluctuation characteristics of rotating fluid machinery are pre-estimated and how the vibration and noise of water pumps are reduced.

MATERIAL AND METHOD

Unsteady numerical calculation program

The steady calculation utilizes the standard k-ε turbulence model; by contrast, the unsteady calculation employs the RNG k-ε turbulence model because this model can handle the high strain rate and substantial flow of a significantly bending flow line while maintaining high calculation efficiency. The RNG k-ε turbulence model was proposed by Yakhot et al. [11] in 1986 and was deduced from the mathematical method of a renormalization group. This model improves on the standard k-ε model to some

拟相结合的测试分析和数值计算研究[4,7,12]。例如：国外文献[2][10][14]研究了泵内叶轮扩散段与泵性能之间的相互影响，发现叶轮出口处的不稳定流动是造成压力脉动的主要原因。文献[3]瑞士的 APRE 等通过试验在设计工况下 6 个不同流量点进行稳态分析，对混流式水轮机模型尾水管内部流动进行了研究，分析尾水管锥管内脉动幅频特性及无汽浊情况小流量点的涡带频率和压力脉动。文献[1]对离心泵出口法兰附近进行了高频压力传感器测量，采集的数据进行了 FFT 变换，结果信号主频为离心泵叶片通过的频率，应用该信号对泵的转速进行了数据测量。文献[13]总结了国内外的压力脉动测试技术，采用试验的方法对离心泵叶轮出口各方向进行了压力脉动特性试验，获得了流体不稳定流动和叶轮出口压力脉动的关系，研究结果表明压力脉动主要成分是射流－尾迹处诱导的叶频脉动及叶轮流道内流动的不对称性诱导的轴频脉动，结构引起的压力脉动幅值随叶轮和蜗壳劈面间距的增大而逐步减弱并在叶轮出口处的压力脉动频谱中发现介于 4 倍轴频到叶频之间的 100HZ~145HZ 的宽带频率。文献[8]CHARLER 应用大涡模拟方法对混流式水轮机蜗壳、转轮和尾水管分别进行了计算，但部分模型是转轮模拟，无法在尾水管入口选择真实的边界条件。虽然选择平均入流条件，尾水管的计算流态仍很不稳定，对于尾水管压力脉动试验主要是压力脉动幅频特性，无法观测其内部，所以计算压力脉动幅值及产生压力脉动相关原因分要是十分必要的。

本文基于三维 N-S 方程，采用 RNG k-ε 湍流模型，以二次变曲率半开离心式农用汽车水泵全流道为研究对象进行非定常数值模拟，分析了在 Q/Qd=0.7、1 及 1.3 三种工况下的全流道非定常压力脉动特性。结果对于研究如何预估旋转类流体机械的压力脉动特性，对减小泵体的振动，降低水泵噪声是具有重大的现实意义。

材料与方法

非定常数值计算方案

在定常计算中，采用的是湍流模型 Standard k-ε 模型，在非定常计算中考虑到 RNG k-ε 湍流模型可以很好地处理高应变率及流线弯曲程度较大的流动，又能够保证较高的计算效率，选用 RNG k-ε 湍流模型。该模型是 1986 年 Yakhot 等[11]提出，它是由重化群的数学方法推导出来，针对标准 k-ε 模型做了一些改进[9]。对于不可压缩、定常流

extent [9]. Given an incompressible and steady flow, the RNG k-ε turbulence model is expressed as:

动的情况，RNG k-ε 湍流模型的表达式如下：

$$\frac{\partial(\rho u_j k)}{\partial x_j}=\frac{\partial}{\partial x_j}(\alpha_k \mu_{ef} f \frac{\partial k}{\partial x_j})+G_k-\rho\varepsilon \tag{1}$$

$$\frac{\partial(\rho u_j \varepsilon)}{\partial x_j}=\frac{\partial}{\partial x_j}(\alpha_\varepsilon \mu_{eff} \frac{\partial \varepsilon}{\partial x_j})+\frac{\varepsilon}{k}(C_1 * G_k-C_2\rho\varepsilon) \tag{2}$$

Through a comparison between the k-ε model and the RNG k-ε model, the latter modifies C_2 in the ε equation of the former:

对比 k-ε 模型和 RNG k-ε 模型可以发现，RNG k-ε 模型对 k-ε 模型中 ε 方程的 C_2 项进行了修正，即：

$$C^*_2=C_2+\frac{C_\mu\rho\eta^3(1-\frac{\eta}{\eta_0})}{1+\beta\eta^3} \tag{3}$$

where： $\mu_{ef}=\mu+\mu_t$； $C_\mu=0.0845$； $\alpha_k=1.39$； $C_1=1.42$； $C_2=1.68$；

式中： $\mu_{ef}=\mu+\mu_t$； $C\mu=0.0845$； $\alpha_k=1.39$； $C_1=1.42$； $C_2=1.68$；

$$C_1^*=C_1-\frac{\eta(1-\eta/\eta_0)}{1+\beta\eta^3}\quad \eta=(2E_{IJ}.Ei_j)^{1/2}\frac{k}{\varepsilon}\quad E_{ij}=\frac{1}{2}(\frac{\partial u_i}{\partial x_j}+\frac{\partial u_j}{\partial x_i}) \tag{4}$$

where： $\eta_0=4.377$,$\beta=0.012$.

C_2 is modified; thus, the coefficient of the eddy viscosity of the RNG k-ε model under a low-strain rate is higher than that of the standard k-ε model but lower under the high-strain rate. The RNG k-ε model considers high-strain rate and substantial curvature flow; this model can achieve significantly higher calculation accuracy than the standard k-ε model can for rotational flow and substantial curvature. The findings are particularly applicable to the calculation of the internal flow of an impeller blade (e.g., axial flow and centrifugal pumps). The RNG k-ε model can generate higher accuracy and reliability in a more extensive flow than the standard k-ε model can because of these characteristics. Thus, the present study adopts the RNG k-ε model.

The entrance, exit, and static wall surface were similar to those for steady calculation. The interface between the inner rotor and the pump stator was set as the transient rotor stator. The steady calculation result was employed as the initial flow field for unsteady calculation.

According to the requirement of the calculation model regarding Courant number.

其中，$\eta_0=4.377$，$\beta=0.012$。

由于对 C_2 进行了修正，使得在低应变率区时 RNG k-ε 模型的湍流涡粘性系数高于标准 k-ε 模型，相反，在高应变率区其湍流涡粘性系数则低于标准 k-ε 模型。由于 RNG k-ε 模型对高应变率以及大曲率过流等因素的影响进行了考虑，所以该模型在运用于旋流和大曲率情况时，能够大大的提高计算精度。对于叶轮叶片(如轴流泵、离心泵等)的内流动计算，该模型尤其适用。上述特点使得在更广泛的流动中，RNG k-ε 模型比标准 k-ε 模型具有更高的精度和可信度。因此，本文采用 RNG k-ε 方程来求解。

进出口及静止壁面设置与定常计算相同，对于泵内转子部件和定子部件之间的交界面，设置为 Transient Rotor Stator，采用定常计算的结果作为非定常计算的初始流场。

由计算模型对库朗数的要求，即:

$$C_o=\frac{|\bar{v}|\Delta t}{l}<100 \tag{5}$$

where Δt is characteristic time; v and l are the characteristic speed and characteristic scale, which were determined based on the estimated mean speed and minimum grid size in this study. The maximum length of the optional time step of this model is 5 ms. Considering the resolution requirements of pressure fluctuation in the high-speed rotating machinery, the final time step length was determined to be 1/90 of the rotation period and the rotating time was set to 4°, that is, approximately 0.11111 ms. Six full periods were calculated under every working condition; the maximum iteration steps of every time step length were set to 10 because of the effective convergence in the steady calculation.

Fig. 1 shows the variable-curvature and half-open prototyping pump and the distribution of monitoring points. P1 is the entrance pressure of the pump; P2–P9 are at the first to eighth cross sections of the volute; P10

式中 Δt 表示特征时间，v 和 l 分别表示特征速度和特征尺度，本文分别取估算的平均速度和网格最小尺寸。本模型可选用的时间步长最大值为 5ms，同时考虑到在高速旋转机械内压力脉动的分辨率要求，最终确定的时间步长为旋转周期时间的 1/90，及 4°的旋转时间，约为 0.11111ms。每个工况均计算 6 个整周期，考虑到在定常计算中收敛性较好每个时间步长最大迭代步数设为 10。

变曲率半开式原型泵及监测点设置如图 1 所示，P1 为泵入口压力，P2 到 P9 位于蜗壳第一断面到第八断面，P10

is close to the water cut of the volute and P11 is at the downstream of the volute; and P12 is the exit pressure of the pump. Considering the positions of the actual pressure-measuring points, all the pressure-measuring points are 2 mm away from the wall surface. Fig. 2 presents the distribution of the testing points and an image of the sensor installation. Fig. 3 provides a panoramic view of the field test system.

The pressure fluctuation coefficient is defined as:

和 P11 位于蜗壳隔舌附近及下游位置，P12 则是泵出口压力。考虑到实际测压点位置，测压点位置都距离壁面位置 2mm 位置。图 2 为试验测点布置及传感器安装实物图，图 3 为现场测试系统全景图。

定义压力脉动系数为:

$$p^* = p_i - \overline{p} \tag{6}$$

where p_i is the simulated transient value of the absolute pressure and $\overline{p}$ is mean pressure in the sample time.

Time coefficient is defined as:

式中 p_i 为模拟绝对压力瞬态值，$\overline{p}$ 为样本时间内的压力平均值。

定义时间系数为：

$$t^* = t_i / T \tag{7}$$

where: t_i is the calculated transient time and T is the rotation period of the impeller, which is 0.01 s in this study.

式中 t_i 为计算瞬态时间；T 为叶轮旋转周期，本文中为 0.01s。

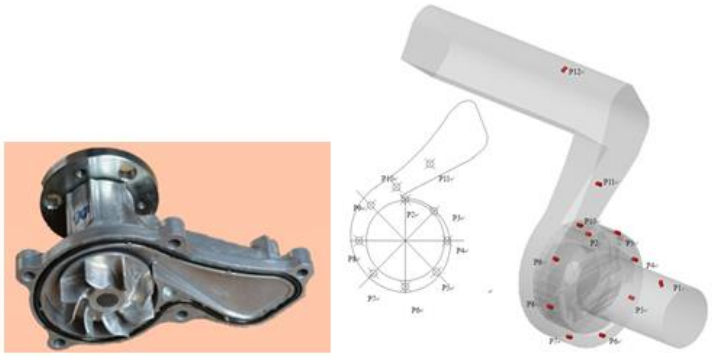

Fig.1- Variable-curvature and half-open prototype pump and the distribution of monitoring points for simulation analysis

Fig.2- Layout of test points and image of sensor installation

Fig.3- Panoramic view of the field test system

RESULTS

Analysis of unsteady external characteristic

Fig. 4 presents the unsteady characteristics of the lift in three periods under different working conditions. The blade positions corresponding to ABCD are marked, and the same blade is highlighted with a red frame. L1 is the start point of the period, and L2 is the end point. This figure 8 shows that:

The unsteady characteristics of a lift change periodically. This change frequency is consistent with the blade passing frequency, and this phenomenon is caused by the dynamic and static interference of the water cut and the impeller. A and B are blade phases indicating that the blade just passes through the water cut. At C and D, the blade is in the middle of the flow passage. Lift fluctuation increases gradually with flow rate. At the same time, the downward pressure fluctuation under a low flow rate exhibited the poorest law in a single period. When flow rate increases, the amplitude change within a single period stabilizes, thereby implying that a high flow rate is conducive to the stable pump operation.

结果

外特性非定常特性分析

图 4 是各工况下在三个周期内扬程的非定常特性，其中标出 ABCD 对应的叶片位置。同一叶片采用红色线框加亮。L1 为周期的起点，L2 为周期的终点。从图中可以看出：

扬程的非定常特性呈现明显的周期性变化，且频率和叶片通过频率一致，这是由于隔舌与叶轮的动静干涉作用引起的。A、B 是叶片相位显示此时叶片恰好掠过隔舌位置，而 C、D 相位显示叶片位于流道中间位置。随着流量的增大，扬程的脉动幅值逐渐增大。同时可以发现，在小流量下的下压力脉动在单周期内的规律性最差，随着流量的增大单周期内的幅值变化逐渐平稳，表明泵的运行稳定性偏向大流量工况。

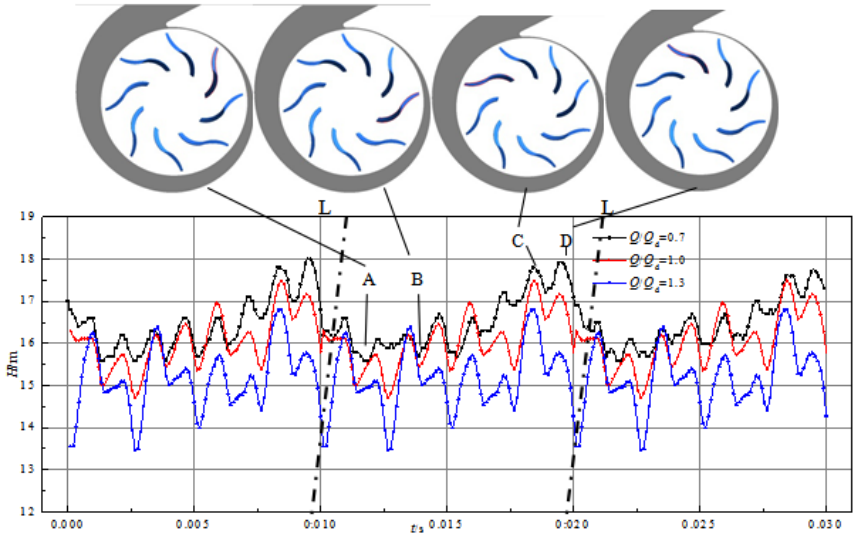

Fig.4- Unsteady characteristics of the lift

Fig. 5 illustrates the static pressure distribution in the middle blade section under the ABCD phases. The minimum and maximum pressures in the middle section fluctuate violently; moreover, the static pressure close to the water cut is relatively higher than that in other positions, as is the lift. A high-pressure gradient appears when the blade exit approaches the flow path of the water cut. When the blade moves to the middle of the flow path, the local high pressure area narrows but pressure increases and the entrance pressure decreases.

图 5 为叶片中间截面在相位 ABCD 下的静压分布，发现在中间截面上的压力的最值有很大的波动，且发现在隔舌附近静压值较高时，扬程出现较高值，当叶片出口边靠近隔舌时，在将要掠过隔舌的流道内出现很高的压力梯度，而当叶片运动到流道中间，局部高压区面积减小，但压力升高，而进口处压力出现降低。

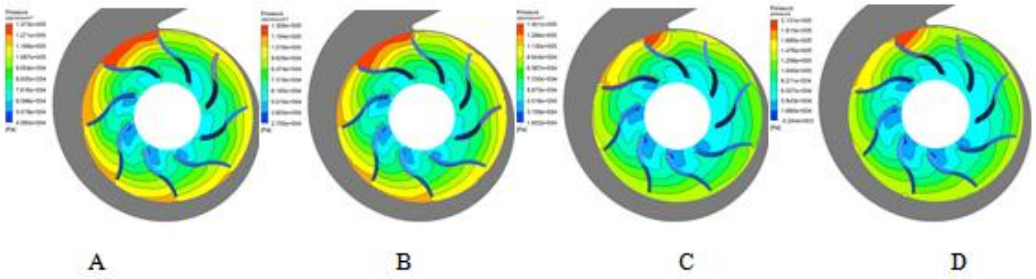

Fig.5- Static pressure at the middle impeller under the ABCD phases

Entrance and exit pressure fluctuations

Fig. 6 presents the time–domain map of pressure fluctuation at the impeller entrance under different working conditions. According to the variation of the pressure fluctuation coefficient, entrance pressure fluctuation does not vary regularly. The minimum pressure fluctuation is achieved under 1.3 Qd, and eight wave peaks occur in a single period. The maximum pressure fluctuation is observed under 1.0 Qd, and a weak correlation exists between pressure fluctuation within a single period and blade frequency. This correlation implies that the optimum working conditions of the pump are skewed to a high flow rate.

进出口压力脉动

图 6 为不同工况下叶轮进口的压力脉动时域图，从图中压力脉动系数的变化可知，在进口的压力脉动规律性不是很明显，在 1.3Qd 工况下压力脉动幅值最小，且在单周期内有 8 个波峰，而在 1.0Qd 工况下压力脉动幅值最大，且单周期内压力脉动与叶频相关性较弱。说明泵的最优工况出现向大流量的偏移。

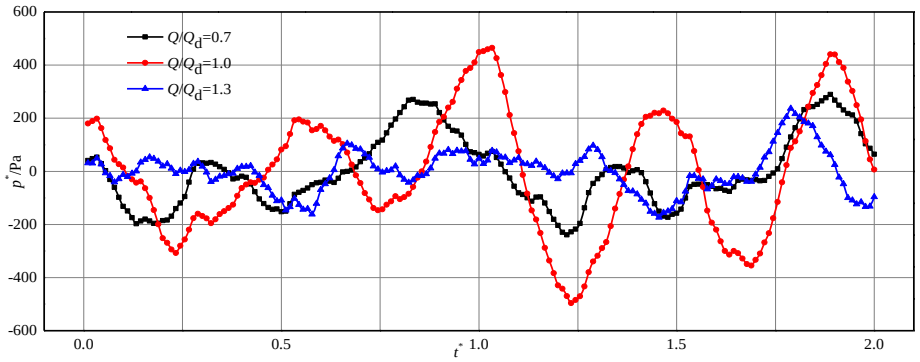

Fig.6- Time–domain map of pressure fluctuation at the impeller entrance under different working conditions

Fig. 7 illustrates the time–domain map of the pressure fluctuation volute exit under different working conditions. Pressure fluctuation at the volute exit is two orders of magnitude higher than that at the impeller entrance; moreover, this pressure fluctuation law is closely related to blade passing frequency. Nonetheless, pressure fluctuation amplitude changes significantly when the impeller is at different phases; the amplitude under different flow rates does not change when the impeller is at the same phase. This outcome occurs because the pressure-measuring points at the exit are downstream of the bend, and the turbulence at the bend disrupts downstream pressure monitoring.

图 7 为不同工况下蜗壳出口的压力脉动时域图，出口的幅值变化比进口高两个数量级，且脉动规律与叶片通过频率相关性较高，但叶轮在不同相位上时的压力幅值变化很明显，在不同流量下，叶轮在相同相位上的压力幅值也并不一致。这是由于出口处的测压点位置布置在弯管下游位置，弯管处的湍动对下游的压力监测产生了扰动。

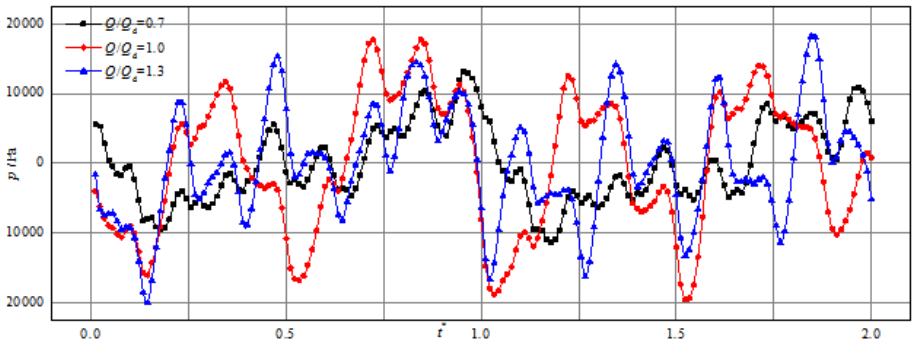

Fig.7-Time–domain map of pressure fluctuation at the volute exit under different working conditions

Pressure fluctuation in volute

Fig. 8 depicts the fluctuations of P2–P9 in two periods. The water cut plays a decisive role in the pressure fluctuation caused by the interaction of the rotating impeller and the static impeller. The water cut is the main pulsation source of pressure fluctuation. In this case, pressure fluctuation amplitude decreases gradually with an increase of flow rate. This result demonstrates that

蜗壳内压力脉动

图 8 为蜗壳内第一断面到第八断面上监测点处的绝对压力在两个周期内的压力脉动，从图中可以看出：

在旋转叶轮与静止蜗壳的相互干涉产生的压力脉动中，隔舌起着绝对作用，是产生压力脉动的主要脉动源，且本

flow stabilizes and the losses caused by internal turbulence decrease with an increase in flow rate. The optimum working condition is skewed to a high flow rate.

Pressure fluctuation differs at various monitoring points on the same volute section. This fluctuation decreases first and then increases from the bottom volute to the back volute. Moreover, many dither components are detected at the monitoring points on the volute bottom. The maximum pressure amplitude along the circumference of the volute is at the monitoring points proximal to the water cut. The distance between the circumferential monitoring points and the water cut increases with the circumference angle, whereas fluctuation amplitude decreases gradually. Two wave peaks in one period are observed on the second, third, and seventh sections, thus indicating that these flow sections experience significant turbulence, which in turn covers the pulsation source of the water cut.

例中，随着流量的增大，压力脉动幅值逐渐减小，表明随着流量增大，流动趋于平稳，内部湍动造成的损失减小，最优工况向大流量工况偏移。

处于同一蜗壳断面不同位置的监测点的压力脉动幅度不同，从蜗壳底部向蜗壳背面先减小后增大，且位于蜗壳底部监测点的高频脉动成分较多。沿蜗壳周向，隔舌附近监测点压力脉动幅度最大，随着圆周角的增加，各监测点沿周向与隔舌距离变大，脉动幅值逐渐减小。

在第二、三及第七断面出现了在单个周期内只有两个波峰的情况，说明在这些过流断面出现了极大的湍动，覆盖了隔舌的脉动作用源。

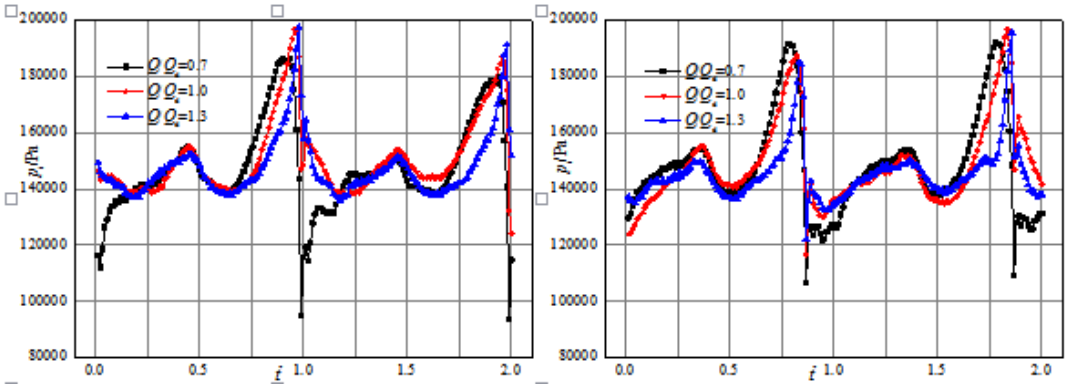

(a) Numerical calculation of the pressure fluctuation at P2 (b) Numerical calculation of the pressure fluctuation at P3

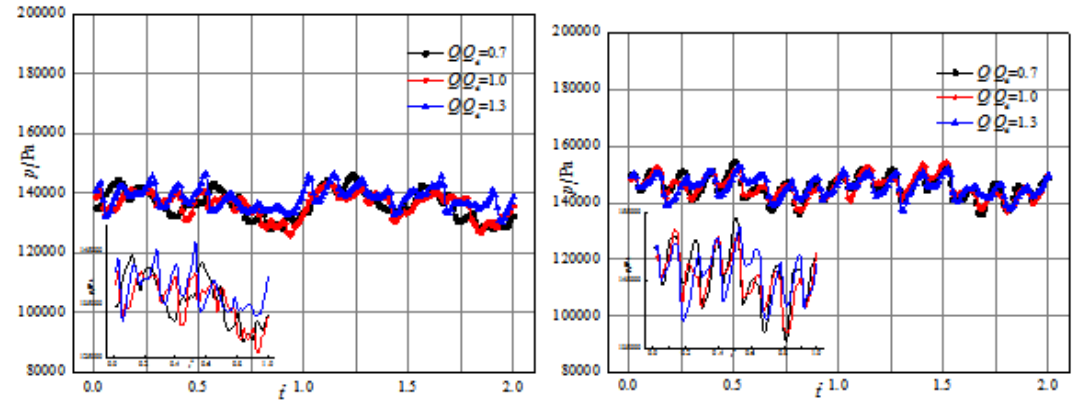

(c) Numerical calculation of the pressure fluctuation at P4 (d) Numerical calculation of the pressure fluctuation at P5

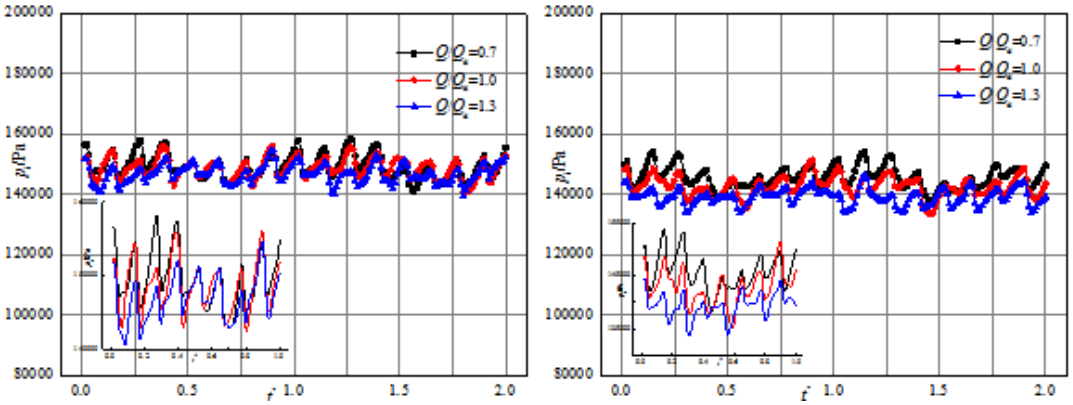

(e) Numerical calculation of the pressure fluctuation at P6 (f) Numerical calculation of the pressure fluctuation at P7

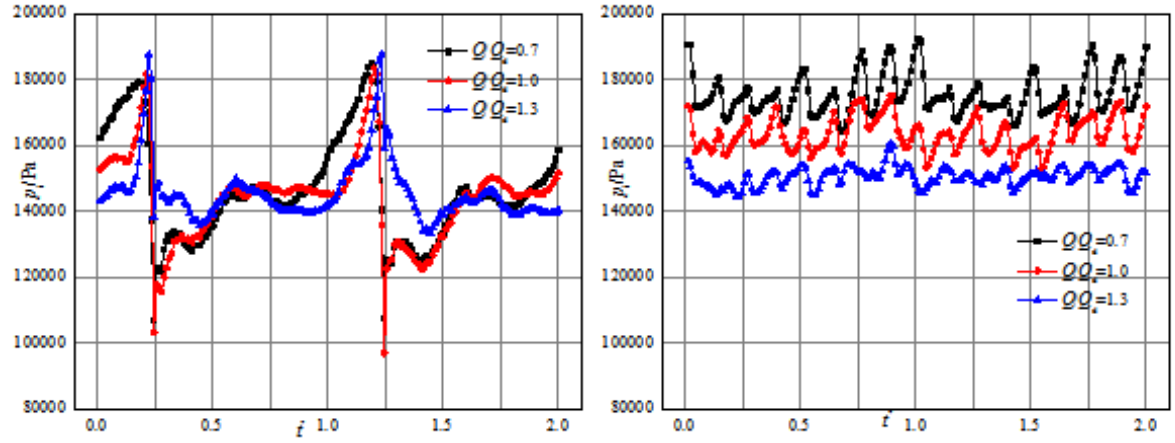

(g) Numerical calculation of the pressure fluctuation at P8 (h) Numerical calculation of the pressure fluctuation at P9

Fig.8-Numerical calculation of the pressure fluctuation in the volute

Pressure fluctuation in the water cut area

Fig. 9 displays the pressure fluctuation at the monitoring points close to the water cut. Generally, mean pressure declines with an increase in flow rate. Meanwhile, the pressure fluctuation law reflects the dynamic and static interference at the water cut. At the same time, the pressure downstream of the water cut is higher than that at a location close to the water cut. In other words, fluid pressure increases from the volute to the volute downstream. The pressure fluctuation at the water cut of the quadratic variable-curvature centrifugal pump differs from the regular pressure fluctuation of a common centrifugal pump, which is in turn positively correlated with the blade number. A significant difference is observed between the adjacent wave peaks of the pressure fluctuation in the quadratic variable-curvature centrifugal pump. Subsequently, the internal flow mechanism is analyzed further through testing.

隔舌区域压力脉动

图 9 是隔舌附近监测点压力脉动，整体而言压力平均值随着流量的上升而下降，而压力脉动的规律体现了隔舌处动静干涉。且隔舌下游的压力在同一时刻高于隔舌附近区域，即在流体进入蜗壳至隔舌下游仍然是增压过程。二次变曲率离心泵的隔舌处的压力脉动区别于普通离心泵的规则的与叶片数正相关的波形图，相邻波峰值之间有较大差值。这一问题需要结合试验手段进一步研究其内部流动机理。

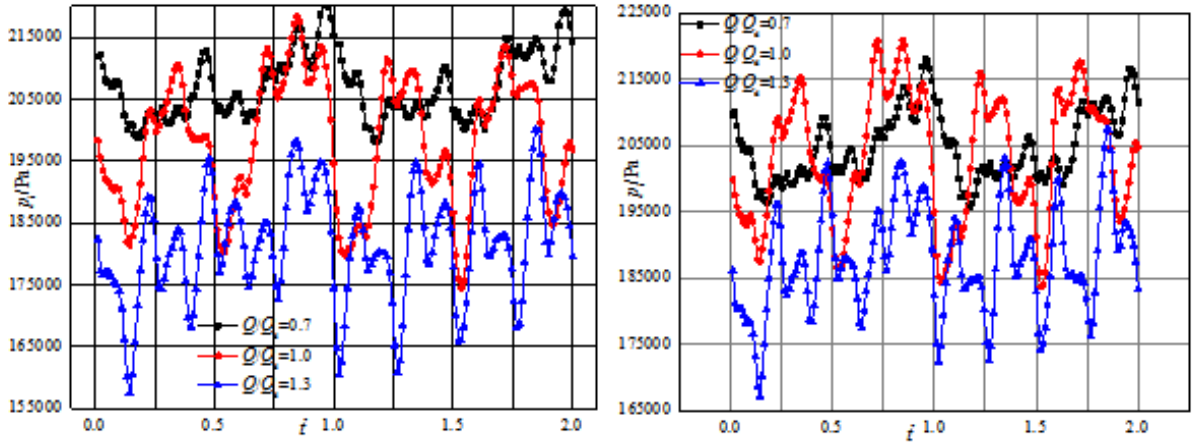

(a) Numerical calculation of the pressure fluctuation at P10 (b) Numerical calculation of the pressure fluctuation at P11

Fig.9-Numerical calculation of the pressure fluctuation near the water cut

Experimental verification

According to the distribution of the actual test points, C4–C8 pressure monitoring points are scattered on the full flow path of the volute. C7 is proximal to the water cut, and this point is the closest one to the outlet. C8 is the most proximal point to the volute exit; meanwhile, C4, C5, and C6 scattered on the volute evenly.

试验验证

按照试验实际测点位置布置，在蜗壳整个流道上分布着 C4~C8 压力监测点，其中 C7 在隔舌附近，离出水口最近，C8 离蜗壳出口最近，C4，C5，C6 均匀分布在蜗壳上。

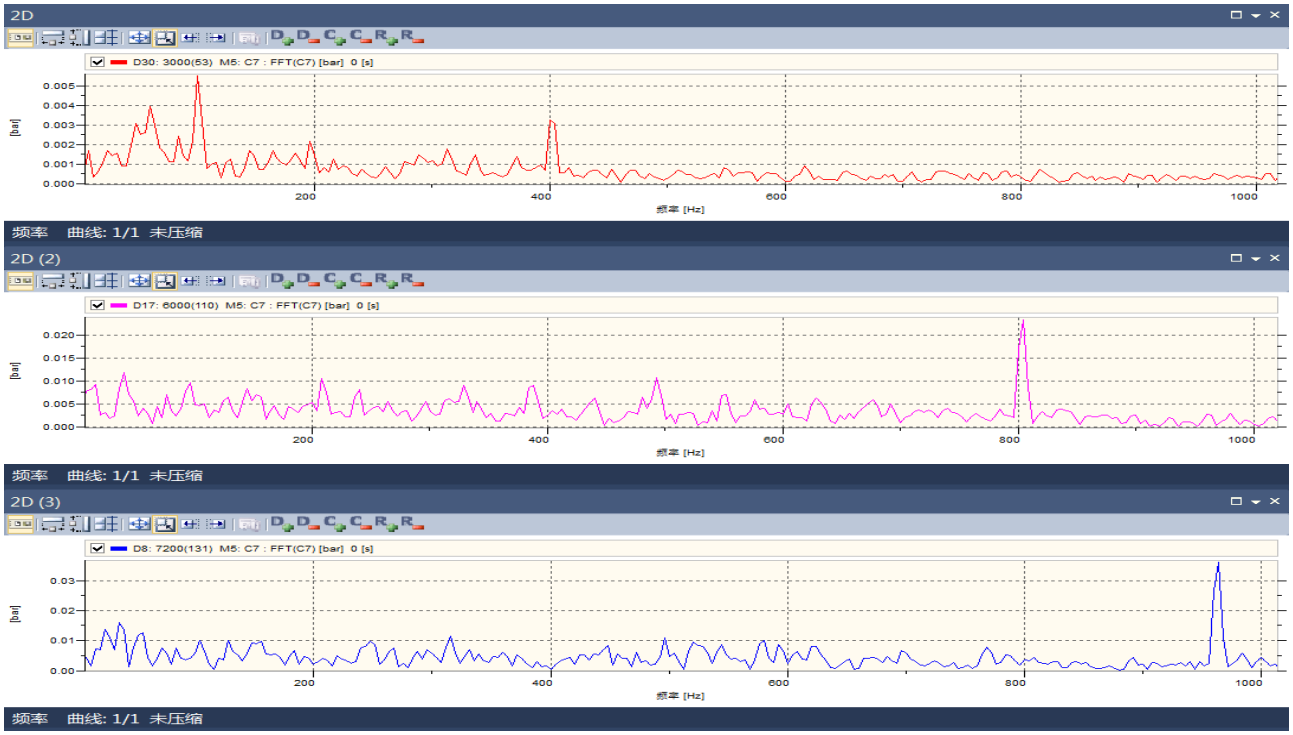

Fig.10-Pressure fluctuation at C7 under different working conditions

Fig.10 indicates that the main frequency component at C7 under different working conditions is the blade passing frequency. Additionally, random fluctuations occur in the low-frequency area. These low-frequency random fluctuations are caused by the secondary flow in the impeller and efflux tail, as with similar to white noise. The pressure fluctuation amplitude is proportional to rotation speed and flow rate. At the same time, the pressure fluctuation under a low flow rate exhibited the poorest law in a single period. Low frequency (< twice that of blade passing frequency) can influence pressure fluctuation significantly because of the turbulence in the pump. As flow rate increases, the changes in pressure fluctuation amplitude within one period gradually stabilize and the random fluctuation declines evidently. This outcome indicates that a high flow rate is beneficial to steady pump operation. This result is consistent with the outcome of the analysis of unsteady external characteristics.

The results for C4, C5, and C6 in Fig. 11 indicate that the pressure fluctuation in the volute flow path is mainly affected by the blade passing frequency. All the monitoring points are primarily influenced by low frequency. The dominant frequency reduces continuously and is minimized at C5 from C7 to C6 and C5, which is close to the water cut. This outcome indicates that the main pressure fluctuation source is the static–dynamic coupling effect at the impeller and the water cut. Based on the results in C4 and C8, the dominant frequency amplitude at locations proximal to C8 is increased and peaks at C8. The dominant frequency is mainly influenced by twice the blade passing frequency. This outcome corresponds to the pressure fluctuation law under normal working conditions. This result is the consequence of the dynamic–static coupling effect of the water cut and the impeller as well as the influence of the right angle outlet of the auto water pump. Although the outlet is far from the pulsation source of the water cut and the dynamic–static coupling effect of fluid in volute is weak, the outlet is close

由图 10 所知，不同工况下测点 C7 主要的频率成分为叶片通过频率。另外在低频区域出现一些随机脉动，这是由于在叶轮中有二次流及射流尾迹的影响，造成的低频随机脉动，类似于白噪声。随着转速及流量的增大，脉动幅值逐渐增大。同时可以发现，在小流量下的压力脉动在单周期内的规律性最差，由于泵内湍流，低于 1 倍叶片通过频率的低频对压力脉动有很大影响，随着流量的增大单周期内的幅值变化逐渐平稳，其随机脉动呈明显减少趋势，表明泵的运行稳定性偏向大流量工况，这与外特性的非定常结果分析一致。

由图 11 C4，C5，C6 可以看出，蜗壳流道内的压力脉动主要受叶片通过频率影响，各监测点主要是低频的影响，从 C7 点隔舌附近到 C6 点、C5 点，主频呈现递减趋势，到 C5 点处最小。这说明压力脉动源主要是叶轮与隔舌处的动静耦合。从 C4、C8 监测点可以看出，离出口 C8 点越近，主频幅值越大，到 C8 点达到最大值，主频主要是 1 倍的叶频影响较大。这与正常工况下的压力脉动规律一致，这主要都是来源于隔舌与叶轮之间的动静耦合，并且与汽车水泵的直角拐角出水口流量冲击的作用。虽然出口离隔舌脉动源较远，蜗壳内液流动静耦合影响较小，但离拐角较近，受到直角冲击，液流分流增强了压力脉动，使得 C8 点

to the corner and bears the direct impact. Fluid separation enhances pressure fluctuation, thus generating the same pulsation intensity at C8 and significantly higher pressure amplitude than the other monitoring points. This outcome conforms to the results of the numerical analysis.

虽离隔舌脉动源较远，压力脉动强度没有出现减小，压力幅值相对其他位置有明显增大，这与数值分析结果相一致

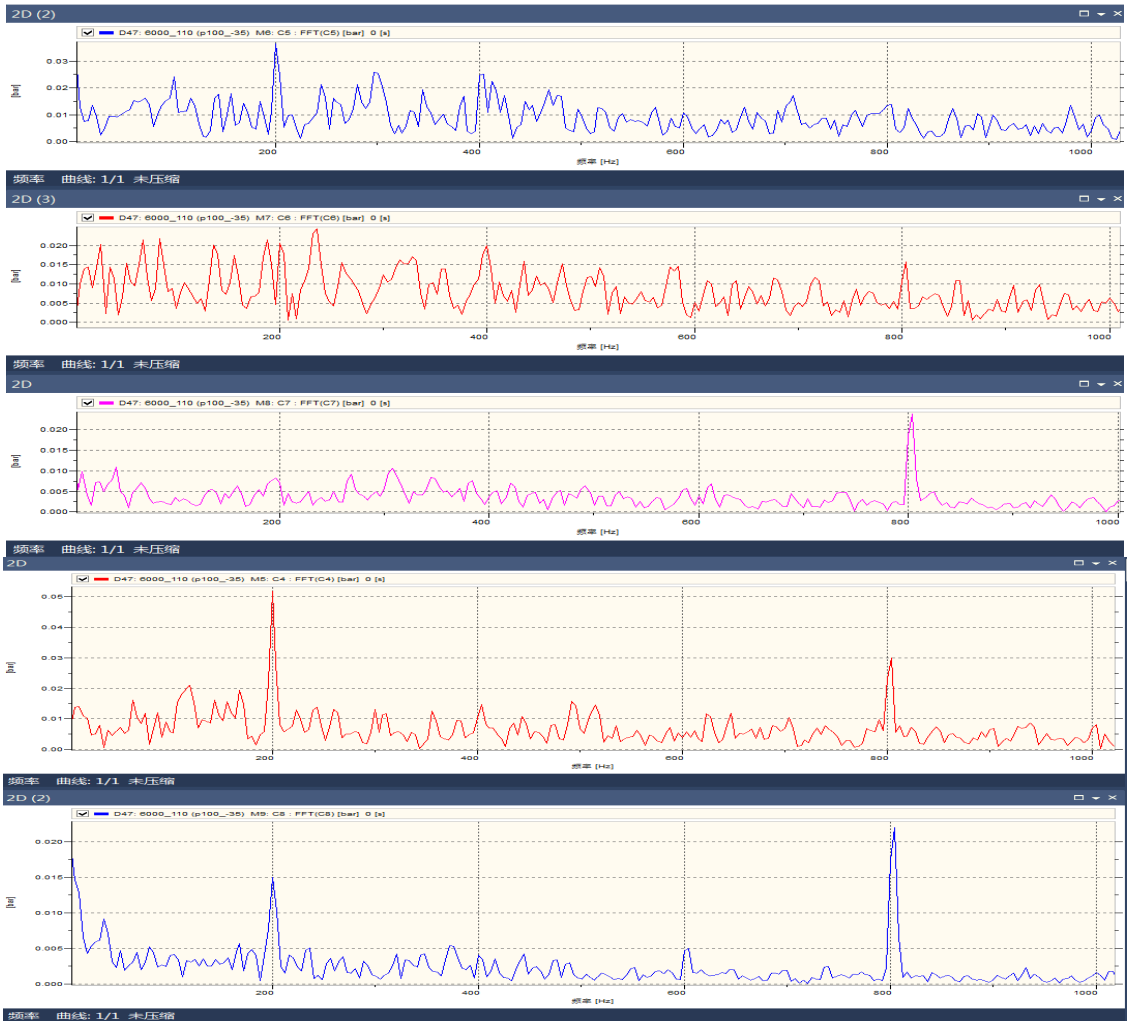

Fig.11 - Frequency spectra of the pressure fluctuations at C4, C5, C6, C7, and C8

CONCLUSIONS

This research conducts an unsteady numerical simulation and experimental study on quadratic variable-curvature and half-open centrifugal agricultural auto water pumps. The findings of this work are significant with respect to the application of analysis and simulation techniques in analyzing the dynamic characteristics of an agricultural auto water pump and in optimizing its structure design to improve the performance of the auto-cooling water pump, to reduce the product development period, and to lower cost. This work concludes that:

(1)The unsteady characteristics of the lift change periodically. This frequency change corresponds with the blade passing frequency, and this outcome is mainly attributed to the dynamic and static interference of the water cut and the impeller. Pressure fluctuation intensifies gradually with an increase in rotation speed and flow rate.

(2)The pressure fluctuation under a low flow rate exhibits the poorest law in a single period. The low frequency (< twice that of blade passing frequency) significantly influences pressure fluctuation because of the turbulence in the pump. As flow rate increases, the

结论

本文对二次变曲率半开离心式农用汽车水泵进行了非定常数值模拟及试验研究，对于分析模拟技术应用于优化设计农用汽车水泵的动态特性分析和结构设计优化上，提高汽车冷却水泵的性能，缩短产品开发周期，降低成本均具有重要的意义。得出如下结论

（1）扬程的非定常特性呈现明显的周期性变化，且频率和叶片通过频率一致，这是由于隔舌与叶轮的动静干涉作用引起的。且随着转速及流量的增大，脉动幅值逐渐增大。

（2）在小流量下的压力脉动在单周期内的规律性最差，由于泵内湍流，低于 1 倍叶片通过频率的低频对压力脉

pressure fluctuation amplitude in a single period gradually stabilizes and the random fluctuation decreases significantly. This result indicates that a high flow rate is beneficial for steady pump operation.

(3)Pressure fluctuation differs at the various monitoring points on the same volute section; this fluctuation decreases first and then increases from the bottom volute to the back volute. Many dither components are detected at the monitoring points at the bottom volute. The monitoring points close to the water cut along the circumference of the volute experience maximum pressure fluctuation. Moreover, the distance between the circumferential monitoring points and the water cut increases with the circumference angle, whereas the pressure fluctuation weakens gradually.

(4)The pressure fluctuation at the water cut of the quadratic variable-curvature centrifugal pump varies from the regular pressure fluctuation of a common centrifugal pump, which is in turn positively correlated with blade number. The differences between adjacent wave peaks are significant; this result conforms to the result of the experimental analysis.

ACKNOWLEDGEMENT

Science and Technology Research Project of Henan Province (142102210555).

REFERENCES

[1]. Aihua Jiang, (2011) - *Research On Vibration Of Centrifugal Pump Base Incited by Fluid Force*, Shang Hai Jiao Tong University;

[2]. Akhras A, Hajem M EI, Champagne J Y, et al., (2004) - *The Flow Rate Influence on The Interaction of a Radial Pump Impeller and The Diffuser, International Journal of Rotating Machinery*, Vol.10, no.4, pp.309-317;

[3]. Arpe J., (2003) - *Experimental Investigation of Unsteady Pressure And Velocity Field in a Draft Tube of Francis Turbine*, EPFL - Laboratory for Hydraulic Machines;

[4]. Chus, Dong R, Katz J., (1995) - *Relationship between Unsteady Flow , Pressure Fluctuation and Noise in a Centrifugal Pump-part B: Effects of Blade-tongue Interactions*, ASME J. Fluids Eng, no.117, pp.30-35;

[5]. Gonzalez J, Fernandez J, Blanco E, et al. (2002) - *Numerical Simulation of The Dynamic Effects due to Impeller-volute in a Centrifugal Pump*, ASME J. Fluids Eng,no.124, pp.348-355;

[6]. Hongjuan Ran, Xianwu Luo, Lei Zhu, et al. (2012) - *Experimental Study of the Pressure Fluctuations in a Pump Turbine at Large Partial Flow Conditions*, Chinese Journal of Mechanical Engineering, no.25, pp.1205-1209;

[7]. Jie Xu, Chuangang Gu. (2004) - *Numerical Calculation of Flow Field in Centrifugal Impeller with Splitter Blades*, Journal Of Chemical Industry and Engineering, vol.55, no.4, pp.541-544;

[8]. Jihong Yin. (1998) - *Numerical Simulation of Francis Turbine Flow by LES Model*, Abroad Large Electric Machine, no.5, pp.60-65;

[9]. Launder B E, Spalding D.B., (1972) - *Lectures in Mathematical Models of Turbulence*, London: Academic Press;

[10]. Shi F, Tsukamoto H. (2001) - *Numerical Study of Pressure Fluctuations Caused by Impeller~diffuser Interaction in a Diffuser Pump Stage*, ASME Journal of Fluids Engineering, vol.123, no.3, pp.466-474;

[11]. Yakhot V, Orszag S A. (1986) - *Renormalization Group Analysis of Turbulence*, Journal of Scientific Computing, no.1, pp.3-11;

动有很大影响，随着流量的增大单周期内的幅值变化逐渐平稳，其随机脉动呈明显减少趋势，表明泵的运行稳定性偏向大流量工况。

（3）处于同一蜗壳断面不同位置的监测点的压力脉动幅度不同，从蜗壳底部向蜗壳背面先减小后增大，且位于蜗壳底部监测点的高频脉动成分较多。沿蜗壳周向，隔舌附近监测点压力脉动幅度最大，随着圆周角的增加，各监测点沿周向与隔舌距离变大，脉动幅值逐渐减小。

（4）二次变曲率离心泵的隔舌处的压力脉动区别于普通离心泵的规则的与叶片数正相关的波形图，相邻波峰值之间有较大差值，这与试验分析结果相一致。

致谢

河南省科技攻关项目资助（142102210555）。

参考文献

[1]. 蒋爱华. (2001) - *流体激励诱发离心泵基座振动的研究*, 上海:上海交通大学;

[2]. Akhras A, Hajem M EI, Champagne J Y, et al. (2004) -*流量对径向泵叶轮和扩散器的影响*, 国际旋转机械杂志, 第 10 卷, 第 4 期, 309-317;

[3]. Arpe J.(2003) - *混流式水轮机的非定长压和流场的实验研究*, 洛桑:洛桑联邦理工学院液压机实验室;

[4]. Chus, Dong R,Katz J. (1995) - *叶片隔舌对离心泵非定常流动、压力脉动与噪声之间的影响*, 美国机械工程师协会.流体工程, 第 117 期, 30-35;

[5]. Gonzalez J, Fernandez J, Blanco E, et al. (2002) - *离心泵叶轮与蜗壳的动力学数值模拟*, 美国机械工程师协会. 流体工程, 第 124 期, 348-355;

[6].冉红娟, 罗先武, 朱磊. (2012) - *涡轮泵局部流动的压力脉动实验研究*, 中国机械工程学报, 第 25 期, 1205 -1209.

[7]. 徐洁,谷传纲.(2004) - *长短叶片离心泵内部流动的数值计算*, 化工学报, 第 55 卷, 第 4 期, 541-544;

[8]. 尹继红.(1998) - 用 LES *法模拟混流式水轮机的水流*, 国外大电机, 第 5 期, 60-65;

[9]. Launder B E, Spalding D B.(1972) - *湍流的数学模型讲座*, 伦敦:学术出版社;

[10]. Shi F,Tsukamoto H.(2001) - *导叶泵叶轮压力脉动扩散的数值模拟研究. 美国机械工程师协会.* 流体工程杂志, 第 123 卷, 第 3 期, 466~474;

[11]. Yakhot V, Orszag S A. (1986) -*湍流的重整化群分析*, 科学计算杂志, 第 1 期, 3-11;

[12]. Zhaohui Xu, Yulin Wu, Naixiang Chen. (2004) - *Unsteady Blade-Row Interaction Calculation in High Speed Pump*, Chinese Journal Of Mechanical Engineering, vol.40, no.3, pp.1-4;
[13]. Zhongyong Pan, Yongyan Ni, Shouqi Yuan. (2010) - *Experiment and Mechanism of Centrifugal Pumps Rotation Speed Measurement Based on Rotor-stator Interaction*, Transactions of the Chinese Society for Agricultural Machinery, vol.41, no.3, pp.81-85;
[14]. ZieglerK U, Gallus H E, Niehuis R. (2003) – *Study on Impeller~diffuser Interaction Part I: Influence On the performance*, Journal of Turbo machinery, vol.125, no.1, pp.173-182.

[12]. 徐朝晖, 吴玉林, 陈乃样. (2004) - *高速泵内三维非定常动静干扰流动计算*, 机械工程学报, 第 40 卷, 第 3 期, 1-4;
[13]. 潘中永, 悦永燕, 袁寿其. (2010) - *基于动静干涉的离心栗转速测量机理与实验,* 农业机械学报, 第 41 卷, 第 3 期, 81-85;
[14]. ZieglerK U, Gallus H E, Niehuis R. (2003) - *叶轮扩散器对部分零件性能的研究*, 涡轮机械杂志, 第 125 卷, 第 1 期, 173-182